

Construction and Characterization of Engineered Bacterial Cell-Cell Communication Modules

Anna Labno,^{*} Barry Canton,[†] and Andrew Endy[‡]

MIT Synthetic Biology Working Group

(Dated: December 15, 2005)

Current research in synthetic biology aims to enable the design and construction of living organisms in the manner that we now engineer electrical, mechanical, and other systems. To facilitate the design of higher-order systems, we need to be able to predict the behavior of a system from the characteristics of the components that might comprise it. Thus, designing and using a methodology for characterizing the performance of biological parts and devices is central to the future success of biological engineering. Here, we engineered a cell-cell communication device based on parts from the quorum sensing system of *Vibrio fischeri*. This receiver responds to the concentration of a small signaling molecule (AHL) in the media by modulating the transcription rate that is output from the device. To begin to systematically characterize the construct, we connected it upstream of a fluorescent protein-based reporter device. Experiments based on multi well fluorimetry measurements, FACSscan and fluorescent microscopy revealed: device INPUT/OUTPUT transfer function (including switch point, latency, and variation across clonal colonies), input signal specificity, and device stability (both genetic and performance). The short latency of the device complemented by long genetic and performance stability makes it suitable for use in wide variety of applications including fast response circuits and continuous operation circuits with 15% or higher tolerance level. This work presents a first attempt at comprehensive characterization of a standard biological part and can be applied to vast majority of genetic devices.

1. INTRODUCTION

Advances in the field of synthetic biology are making it feasible to engineer biological systems. Current research aims to make it possible to engineer biology in the manner that we currently engineer electrical or mechanical systems. Elements such as logic gates and oscillators have already been constructed using genetic and biochemical components [1, 2]. However, biological systems offer properties and functions not found in traditional engineering systems, such as the ability to survive in a variety of conditions and extreme sensitivity to changes in surroundings. They can produce antibiotics, enzymes, medicines and other useful chemicals very efficiently due to their self-replicating nature. Specially programmed cells could monitor our bodies for early signs of problems, for example, monitoring blood sugar concentrations or cholesterol buildup in arteries.

A crucial part of system design is predicting its behavior based on the specification of constituent components. Use of standardized, interchangeable and specified components makes this possible just as has occurred in electronic circuit design. MIT has already begun to assemble a library of such genetic circuit building blocks [3]. Such a library will allow the design of families of these devices with different performance characteristics by varying module components. Cell-cell communication is a key capability that will allow individual cells to coordi-

nate their behavior with the rest of the population. This coordinated behavior permits consensus decisions, which allows the formation of spatial patterns and the accomplishment of more complex tasks [4–6]. To make this outcome a reality, however, we must first develop an engineering methodology for designing biological systems as well as for deepening our understanding of cell-cell communication and ability to harness it.

We engineered and comprehensively characterized a component of a cell-cell communication device: a receiver device. A receiver device is one that responds to the presence of a signaling molecule in the extracellular media (autoinducer) by increasing transcription from a promoter. The design was based on elements of the quorum sensing system of *Vibrio fischeri*. LuxI is the autoinducer synthase that is responsible for the synthesis of the acyl-AHL autoinducer N-(β -ketocaproyl)homoserine Lactone (AHL). LuxR is the transcriptional activator protein that, when bound to autoinducer, promotes transcription of the luciferase structural operon *luxCDABE* [7, 8].

We have attached a green fluorescent protein (GFP) gene downstream of the receiver to be able to measure the rate of transcription indirectly through GFP levels. The behavior of this device was represented by a transfer curve, where the input to the device is the AHL concentration and the output of the device is GFP concentration. We measured device variability, which describes how different colonies from a long-term store vary in performance, i.e., how their transfer functions and DNA sequences differ. We measured the level of transcription from induction by AHL derivatives to determine how specific the receiver is to its cognate inducer molecule. In addition, the time it takes for the construct to respond

^{*}Electronic address: labnoa@mit.edu

[†]Electronic address: bcanton@mit.edu

[‡]Electronic address: drew@mit.edu

after induction was measured; we refer to this time delay as the latency of the device. We have also assessed genetic and performance stability of the construct under full-load working condition and no-load working conditions. A mathematical model describing operation of device was formed based on our understanding of biological processes. This model allowed us to calibrate output of the device in terms of a standard unit of biological measurement, Polymerases Per Second (PoPS) rather than relative GFP units, to obtain a more direct way of assessing the level of transcription [9].

This work presents a first attempt of comprehensive characterization of a standard biological part. As such it has a multi-fold importance. In the process of characterizing the LuxR based receiver, we lay out the basis of an engineering methodology for the future characterization of other synthesized biological parts. This methodology describes devices in terms of transfer curves, threshold levels, response times, genetic stability and the dependence of device performance on its components. This methodology can be applied to vast majority of genetic devices and will allow modeling, design and assembly of modules into higher order predictable systems, organizing and directed design of new BioBrick parts, as well as comparison of existing parts between institutions. Availability of full characterization of LuxR receiver makes it ready to be used in a systematic fashion outlined above. Simultaneously this work deepens understanding of the principles underlying the biochemical processes of *quorum sensing* and transcriptional control in cell-cell communication devices. Most importantly, we developed mathematical model describing transcriptional control and experimentally assessed evolutionary changes of the inducible transcription system under different working conditions. Our model is fully supported by experimental data.

2. MATERIALS AND METHODS

In order to comprehensively characterize a receiver device, it was placed in *E. Coli* upstream of GFP reporter. Assays measuring devices specificity to the inducer molecule, variability and latency based on multi-well fluorimeter measurements were conducted. Evolutionary stability was assayed on single cell as well as culture level using multi-well fluorimeter, FACSscan and sequencing tools

2.1. Bacterial strains and plasmids

E. coli strain MG1655 was used in all experiments. T9002 was constructed by BioBricks standard assembly [3]. It consists of a LuxR coding region placed downstream of a tetR controllable $P_{L\alpha}$ promoter and standardized RBS. A standard transcriptional terminator was placed downstream of the LuxR coding region followed

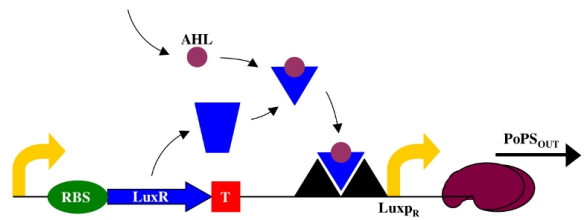


FIG. 1: A schematic of device operation. The AHL molecule is recognized by a member of the LuxR protein family, subsequently AHL-LuxR complex binds to an operator site upstream of a LuxpR family promoter and activate transcription of the downstream gene.

by a LuxpR promoter. For characterization purposes, a GFP production device was placed immediately downstream of the receiver device. The GFP production device consists of a standardized RBS, GFP coding region and a standardized terminator. The combined receiver and reporter device was cloned into plasmid pSB3K3-1[3]. This low copy plasmid has a p15A ori and confers kanamycin resistance. The multiple cloning site (MCS) is flanked by two terminators to prevent any transcription entering from outside the device (FIG1).

2.2. Specificity, Variability and Latency measurements

For the measurements of specificity, variability and latency, 5ml cultures inoculated from a single colony were grown for 15hrs in defined medium (M9 salts Bio 101 Inc.) + 0.005% (w/v) Casamino acids + 0.1% (v/v) glycerol + 2nM $MgSO_4$ + 0.1mM $CaCl_2$ + kanamycin (20 μ g/ml) at 37 $^{\circ}$ C with shaking at 70 rpm. Cultures were diluted 1:1000 into fresh medium and allowed to grow for an additional 5 hours under the same conditions. 200 μ l of the culture was transferred into flat-bottom 96 well plates (Greiner). Wells were pre-filled with the appropriate inducer molecule. These plates were used to grow the cultures in a Wallac Victor3 multi-well fluorimeter at 37 $^{\circ}$ C and assayed with an automatically repeating protocol of absorbance measurements (600nm filter, 0.1 second absorbance through approximately 0.5cm of fluid), fluorescence readings (488nm excitation filter, 525nm emission filter, 0.5 second, CW lamp energy 12902 units), and shaking (1 mm, linear, normal speed). One well was filled with M9 media in all experiments as a background measurement. Time between measurements

was 3 minutes. For the specificity measurements, wells were pre-filled with N-(β -Ketocaproyl)-DL-homoserine lactone, (AHL) and its derivatives 5 to yield 8 different final concentrations: 0nM, 0.01nM, 0.1nM, 1nM, 10nM, 100nM, 1 μ M, 10 μ M. In order to measure device performance variability, cultures were inoculated from 8 individual colonies. Each of the 8 cultures were induced with the same 8 concentrations of AHL. The performance latency of the receiver and reporter system was measured by preparing a culture in the same way as for specificity measurements; however, time between measurements was reduced to 1min in order to obtain better temporal resolution.

2.3. Evolutionary Stability Measurements

The evolutionary stability of the device was tested under two distinct conditions: full working load, which is defined as saturating concentration of AHL, and no load, when no AHL is present. The Cultures were propagated for 5 days; the genetic and performance stability assays were performed daily.

2.3.1. Culture Propagation

Two 5ml cultures were inoculated from the same colony and grown overnight in M9 medium at 37°C with shaking at 70 rpm. One culture had a saturating concentration of AHL (100nM) added. Cultures were diluted 1:400 into fresh medium. The saturating concentration of AHL was maintained. Cultures were further grown under the same conditions for an additional 10h. A 1:4096 dilution was performed and the saturating concentration of AHL was maintained. The cultures were then allowed to grow overnight. This propagation was maintained for 5 days.

2.3.2. Genetic Stability Assay

After the overnight 37°C incubation of cultures, bulk plasmid DNA from each of the cultures was purified using a Qiagen Spin Miniprep Kit and sequenced at Biopolymers Lab at MIT using primers internal and external to the receiver device and reporter device [10]. VectorNTI 7.1 (Invitrogen) was used for analyzing the resulting sequences.

2.3.3. Performance Stability Assay

A second copy of 1:400 dilution of the overnight was made. These second copies were grown in the absence of AHL for 8hrs. This step was to eliminate any accumulated GFP molecules before assaying performance. Samples were transferred into flat-bottom 96 well plates

at a final volume of 200 μ l per well, and assayed using a Wallac Victor3, as described above for the specificity measurement. Samples from both of the cultures were also incubated for 45mins with eight standard AHL concentrations at 37°C with shaking at 70 rpm. They were assayed immediately afterwards using FACS. Single-cell fluorescence measurements were carried out on a Becton-Dickinson FACScan flow cytometer with a 488-nm Argon excitation laser and 525-nm emission filter. FACScan data were analyzed using Cell Quest and FlowJo. During each flow-cytometer measurement, data was collected from 50000 cells. 2 μ l of Sphero fluorescent beads (0.87 μ mo) in 500 μ l H₂O were used as a control for temporal variation of cytometer variation.

2.4. Data Analysis

Raw measurements of absorbance and fluorescence from the Wallac were processed by subtracting the absorbance of the media and fluorescence respectively from all samples. Absorbance was then converted to OD600. The change in the background corrected fluorescence per OD was calculated per time step and averaged over three time points. The running average was taken as being proportional to the rate of accumulation of GFP per cell. This parameter was seen to reach steady state 30mins after induction. The running average was further converted into a final output of PoPS using equation 4.

3. RESULTS

3.1. Methodology of Characterization

The ability to engineer both prokaryotic and eukaryotic cell-cell communication systems will be central to the future engineering of population-level biological systems. However, to make this process feasible, a comprehensive characterization scheme is necessary. The transfer function from device input to output is the primary characteristic of a cell-cell signaling modules. For the receiver device, the input signal is concentration of the inducer molecule. The output of the device is polymerizes per second (PoPS). We can derive certain parameters that capture the key characteristics of the transfer curve - Hi/Lo values, noise level and the switch point of the device. We defined and fully characterized a receiver device. The response of the device to 8 different concentrations of inducer molecule were used to produce the device transfer function (Figure 3).

The maximum level of this output was determined to be 12000 GFP rate/ absorbance and was observed above AHL concentration of 10-7M. The device was considered to be off (Lo value) when GFP production was below 10 % of the maximum output, which occurred below 10-9M AHL. We believe that the most important characteristics of this device are its degree of specificity to a range

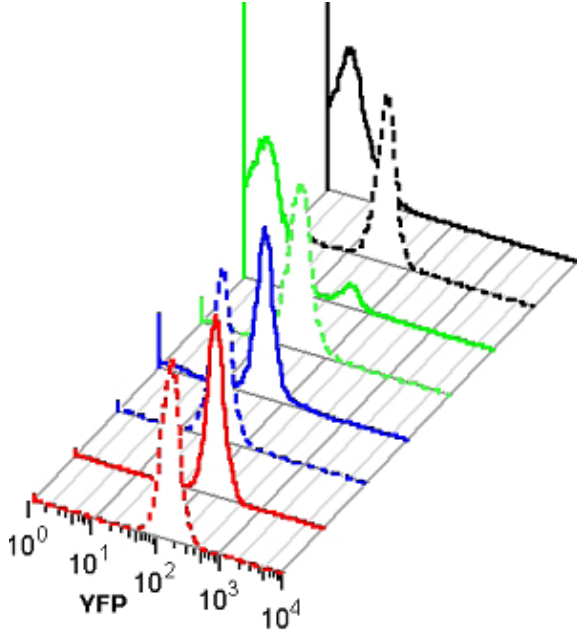


FIG. 2: FACS data acquired during four days of stability experiment (day 1 —, day2 —, day3 —, day4 —) representing number of cells expressing YFP with a given intensity (arbitrary units). Cultures propagated without AHL (dashed lines) maintain uniform YFP expression over the course of experiment while those that were propagated under full load condition (solid lines) i.e 100nM AHL become mostly unable to express YFP in the third day of the experiment.

of inducer molecules, variability of performance between genetically identical colonies, latency and evolutionary stability. Each of these characteristics was investigated and results are summarized in following sections.

3.2. Specificity

We sought to quantify the ability of the device to distinguish between its cognate inducer AHL (N-(β -Ketocaproyl)-DL-homoserine lactone) and a range of chemically similar inducers (shown in Table 1). Figure 2 shows transfer curves obtained using the different AHL molecules as inputs. The maximal output of the device (Hi level), which is present at concentrations of inducer above 10^{-7} M, shows strong dependence on the specific inducer. Optimal operation with output level of 13000 GFP rate/output is only achieved by using the cognate AHL. The same inducer but lacking a carbonyl group and having chain length intact or extended to 7, 8 or 10 carbon atoms show response decreased by less than 10 % with respect to optimal output. When the AHL molecules have their side chains extended further to 12 carbon atoms or shortened to 4 atoms, activation is visible, but its level is only around 15-20 %. When the side chain backbone consists of 14 carbon atoms, there is no device activation. It can be seen that detection thresh-

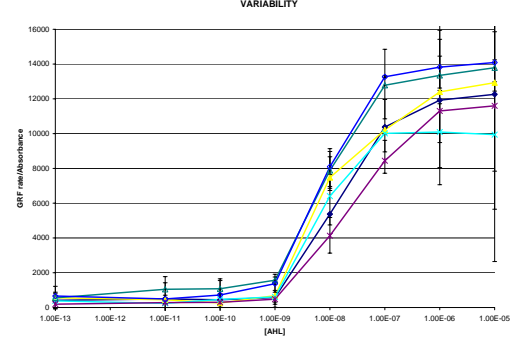


FIG. 3: Transfer functions describing how the output rate of GFP/Absorbance varies with the input concentration of cognate AHL for five different colonies (\triangle , \diamond , \blacktriangle , \blacklozenge , \times , \times) taken from the same long-term storage. Transfer curves have been measured using Wallac Victor3 multi-well fluorimeter.

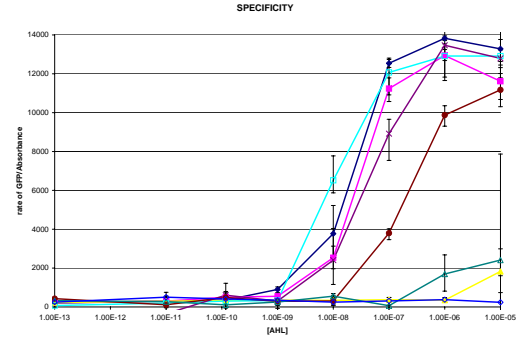


FIG. 4: Transfer functions describing how the output rate of GFP/Absorbance varies with the input concentration of cognate AHL (\blacklozenge) and its various derivatives (see Tab.1). N-Octanoyl-DL-homoserine lactone (\times), N-Hexanoyl-DL-homoserine lactone (\blacksquare), N-Heptanoyl-DL-homoserine lactone (\square), and N-Decanoyl-DL-homoserine lactone (\circ) achieve outputs levels comparable to cognate autoinducers, while N-Butyryl-DL-homoserine lactone (\blacktriangle), N-Dodecanoyl-DL-homoserine lactone (\triangle), N-Tetradecanoyl-DL-homoserine lactone (\diamond) can be considered uninducible. Regardless of the type of autoinducer switch point remains 1.00nM. Transfer curves have been measured using Wallac Victor3 multi-well fluorimeter.

old for each of AHL variations is constant at $\approx 10^{-9}$ M. Below this threshold, there is a regime where the device is always off. This regime does not display significant variations correlated to the type of AHL molecule used.

Name	Structural Formula	Name	Structural Formula
N-(β -Ketocaproyl)-DL-homoserine lactone (cognate)		N-Octanoyl-DL-homoserine lactone	
N-Hexanoyl-DL-homoserine lactone		N-Decanoyl-DL-homoserine lactone	
N-Butyryl-DL-homoserine lactone		N-Dodecanoyl-DL-homoserine lactone	
N-Heptanoyl-DL-homoserine lactone		N-Tetradecanoyl-DL-homoserine lactone	

FIG. 5: Structures of different autoinducers sharing a common homoserine lactone moiety.

3.3. Variability

We measured the performance variation between genetically identical colonies taken from long-term storage. The switch point is sharply defined at 10^{-9} M AHL and consistent between colonies. The average performance of those 8 colonies is 12000 GFP rate/absorbance. The coefficient of variation among the 8 colonies is 15% and is evenly distributed above and below the mean. Other tested concentrations show much lower variation, with coefficient of variation below 10%.

3.4. Latency

Latency is defined as the time lag between a change in input concentration and the output level reaching 95% of its final value. These values were obtained by measuring the rate of GFP accumulation at a high induction level every minute until steady rate was obtained (Figure 4). The rate is steadily increasing reaching the plateau of 12000 GFP rate/absorbance after 40min. This implies latency of 23min for the receiver-reporter construct.

3.5. Evolutionary Stability

Evolutionary stability was investigated in order to estimate long-term device performance under different operating conditions. Bulk performance under no-load conditions shows slight variations in GFP production through the course of experiment (coefficient of variation less than 15). Performance of the device working under full load conditions does not show variations during first two days of the experiment; however, in the third day Hi level dropped to approximately a half of original level and on day 4 the device could not be activated at all. In

order to gain more insight into mechanism of failure, single-cell performance was investigated using FACSscan and showed that the population of cells split on day 3 into two groups: a large one, which was not fluorescent and a much smaller one, which still retained fluorescence. On the last day there weren't any visibly fluorescent cells. DNA sequence remained unchanged when device was operated without any load. When operated under saturating condition, on Day 3, when populations separated, cells acquired a mutation in the receiver sequence that was in the coding region and changed Alanine to Valine. On day 4 there were numerous non-silent point mutations in GFP reporter part of the device.

4. DISCUSSION

4.1. Mathematical Model

Based on the understanding of the *Vibrio fischeri* system, we formed a mathematical model which allowed us to infer transcription rate independent of the reporter molecule and plasmid copy number (PoPS) from plate reader fluorescence measurements. This model is implemented in the calibration procedure of multi well fluorimeter Victor3 [11], which relates relative fluorescence measurements from the plate reader to copies of a fluorescent reporter per well. Previous work [12] has shown that absorbance measurements from the fluorimeter can be related to colony forming units (cfu). Assuming these calibrations have been done, we can use the protein copy measurements as an input to a simple model relating protein production rate to PoPS/cfu. This calculation assumes standard model of protein production within a single cell consisting of two coupled differential equations, one governing the rate of accumulation of reporter mRNA per cell and the other governing reporter protein accumulation per cell.

$$\dot{[M]} = k_M[D] - \gamma_M[M] \quad (1)$$

$$\dot{[P]} = k_P[M] - \gamma_P[P] \quad (2)$$

where $[M]$ is the reporter mRNA concentration per cell ($[mRNA]$), $[P]$ is the reporter protein concentration per cell ($[Protein]$), $[D]$ corresponds to the reporter DNA molecule concentration per cell ($[DNA]$), k_M is mRNA production rate in PoPS ($[mRNA][DNA]^{-1}s^{-1}$), k_P is protein production rate in RiPS ($[Protein][mRNA]^{-1}s^{-1}$), γ_M is the mRNA degradation rate (s^{-1}) and γ_P the protein degradation rate. This value, for stable protein such as GFP is equal to the dilution rate due to growth (s^{-1}). Since both the mRNA degradation and production rates are high ($\approx 1min$), we assume that reporter mRNA levels are in pseudo steady state. Hence, we can solve Eqn. 1 to yield

$$M = \frac{1}{k_P} ([\dot{P}] + \gamma_P[P]) \quad (3)$$

This gives a relation between PoPS and protein levels and the rates of production [13].

$$k_M = \frac{\gamma_M}{k_D[D]} \left([\dot{P}] + \gamma_P[p] \right) \quad (4)$$

The rate of the mRNA production and hence the protein production rate is a function of the AHL concentration and its functional form is depicted by transfer function 3. The output function describing behavior of the device is in closed form in all biologically feasible domains and hence can be utilized in simulation programs such as BioSpice [14].

4.2. Cell-Cell Communication Device-Characteristics

We engineered and comprehensively characterized a receiver device in order to provide users with a characteristic of the device sufficient to model it and incorporate into higher level systems. Mathematical model in which the acyl-AHL autoinducer N- β -ketocaproyl homoserine Lactone (AHL) concentration is related directly to the transcription level is consistent with data and accurately predicts the transcription of the luciferase structural operon *luxCDABE* under various induction levels.

The receiver device was shown to be activated by 10^{-9} M AHL and achieved full operating output at 10^{-7} M. It was demonstrated that the clonal colonies do not display a variation in triggering concentration of AHL, and their PoPS production rate at full induction varies by less than 15%. Thus, 15% is a suggested tolerance level for the higher order circuits using this device. Maximum output of the device exhibits strong dependence on the type of the inducer used. While response to cognate AHL molecule lacking a carbonyl group and having chain length intact or extended to 7, 8 or 10 carbon atoms remains within the suggested tolerance level, there is no sig-

nificant induction when the AHL side chain is extended further or shortened. Receivers based on these molecules are not expected to show significant amount of cross talk and can be regarded as orthogonal. Short latency of the device as compared with the cells' doubling time, complemented by long genetic and performance stability, makes it suitable for use in wide variety of applications, including fast response circuit and continuous operation circuits.

4.3. Device Performance-Methodology

A crucial part of system design is predicting the behavior of its constituents based on their specification. We presented here a characterization scheme that can be used to describe a variety of devices. The behavior of many, if not all, devices can be accurately and conveniently represented by a transfer curve, which presents the relation between the input and output of a linear time-invariant system. A common signal carrier for gene expression and a standard unit of measurement was chosen to be polymerizes per second (PoPS) as this makes the characteristic independent of reporter molecule and plasmid copy number. Transfer functions can easily be combined, especially with use of numerical methods, in order to determine joint output of many devices and simulate behavior of more complex systems. Additionally, each device should have well characterized the intrinsic variability between clonal colonies, switch point, latency, input signal specificity and device stability (genetic and performance). We hope that the biological engineering community will begin to work together to populate a library of well-characterized devices in a manner similar to that described here, and propose that a standards committee for device characterization be started to support such work.

-
- [1] R. Weiss, S. Basu, S. Hooshangi, A. Kalmbach, D. Karig, R. Mehreja, and I. Netravali. Genetic circuit building blocks for cellular computation, communications, and signal processing. *Natural Computing, an International Journal*, (2):47 84, 2003.
 - [2] R. Weiss and T. J. Knight. Engineered communications for microbial robotics. In *Proceedings of the Sixth International Meeting on DNA Based Computers (DNA6)*, 2000.
 - [3] see BioBricks at parts.mit.edu
 - [4] B. Bassler. How bacteria talk to each other: Regulation of gene expression by quorum sensing. *Current Opinion in Microbiology*, 2(6):58 587, 1999.
 - [5] K. Nealson. *Cell-Cell Signaling in Bacteria*, chapter Early Observations Defining Quorum-Dependent Gene Expression. American Society for Microbiology, Washington, D.C., 1999.
 - [6] P. Nilsson, A. Olofsson, M. Fagerlind, T. Fagerstrom, S. Rice, S. Kjelleberg, and P. Steinberg. Kinetics of the ahl regulatory system in a model biofilm system: How many bacteria constitute a "quorum"? *Journal of Molecular Biology*, (309):631 640, 2001.
 - [7] J. James, P. Nilsson, G. James, S. Kjelleberg, and T. Fagerstrom. Luminescence control in marine bacterium *Vibrio Fischeri*: An analysis of the dynamics of lux regulation. *Journal of Molecular Biology*, (296):1127 1137, 1999.
 - [8] J. Engebrecht, K. Nealson, and M. Silverman. Bacterial bioluminescence: isolation and genetic analysis of functions from *Vibrio Fischeri*. *Cell*, (32):773 781, 1983.
 - [9] In this process we used unpublished mRNA expression data obtained by Caitlin Conboy.
 - [10] Sequences for those primers (VR1, VF2, C62VF and C62VR) can be found at parts.mit.edu
 - [11] http://openwetware.org/wiki/Standardized_GFP_quantification

- [12] http://openwetware.org/wiki/Endy:Portable_spec
- [13] mRNA degradation rates and RiPS for GFP have been measured by Jeniffer Braff and Caitlin conboy (unpublished data)
- [14] www.biospice.org

Acknowledgments

The authors would like to acknowledge help from N.Lerner and J.K. Kominiarczuk in reviewing the early copies of the manuscript.